

Alma Mater Studiorum Università di Bologna
Archivio istituzionale della ricerca

Spectroscopic detection of the gallium methylene (GaCH_2 and GaCD_2) free radical in the gas phase by laser-induced fluorescence and emission spectroscopy

This is the final peer-reviewed author's accepted manuscript (postprint) of the following publication:

Published Version:

Smith, T.C., Tarroni, R., Clouthier, D.J. (2024). Spectroscopic detection of the gallium methylene (GaCH_2 and GaCD_2) free radical in the gas phase by laser-induced fluorescence and emission spectroscopy. THE JOURNAL OF CHEMICAL PHYSICS, 160, 1-14 [10.1063/5.0182504].

Availability:

This version is available at: <https://hdl.handle.net/11585/956630> since: 2024-02-11

Published:

DOI: <http://doi.org/10.1063/5.0182504>

Terms of use:

Some rights reserved. The terms and conditions for the reuse of this version of the manuscript are specified in the publishing policy. For all terms of use and more information see the publisher's website.

This item was downloaded from IRIS Università di Bologna (<https://cris.unibo.it/>).
When citing, please refer to the published version.

(Article begins on next page)

Spectroscopic Detection of the Gallium Methylene (GaCH_2 and GaCD_2) Free Radical in the Gas Phase by Laser-Induced Fluorescence and Emission Spectroscopy

by

Tony C. Smith,¹ Riccardo Tarroni² and Dennis J. Clouthier^{1a)}

¹Ideal Vacuum Products, LLC, 5910 Midway Park Blvd. NE, Albuquerque, New Mexico 87109,
USA

²Dipartimento di Chimica Industriale “Toso Montanari”, Università di Bologna, Viale
Risorgimento 4, 40136 Bologna, Italy

^{a)}**Author to whom correspondence should be addressed:** djc@idealtvac.com

ABSTRACT

GaCH₂, a free radical thought to play a role in the chemical vapor deposition of gallium-containing thin films and semiconductors, has been spectroscopically detected for the first time. The radical was produced in a pulsed discharge jet using a precursor mixture of trimethylgallium vapor in high pressure argon and studied by laser-induced fluorescence and wavelength resolved emission techniques. Partially rotationally resolved spectra of the hydrogenated and deuterated species were obtained and they exhibit the nuclear statistical weight variations and subband structure expected for a $^2A_2 - ^2B_1$ electronic transition. The measured spectroscopic quantities have been compared to our own *ab initio* calculations of the ground and excited state properties. The electronic spectrum of gallium methylene is similar to the corresponding spectrum of the aluminum methylene radical which we reported in 2022.

I. INTRODUCTION

Gallium-containing compound semiconductors, such as GaAs, GaN, GaP, GaSb, InGaAs, InGaN, AlGaInP, InGaP and AlInGa are important in devices as diverse as infrared laser sources, light-emitting diodes, radiation detectors, solar cells and in the fabrication of quantum wells, wires and dots. Trimethylgallium (TMGa) is the preferred source of gallium for metalorganic chemical vapor deposition (MOCVD) of single- or polycrystalline thin films in which the precursor is decomposed at the hot surface of a substrate. Although extensively employed in industry, the detailed mechanisms of the gas- and gas-surface phase chemical reactions that take place in gallium MOCVD are still poorly understood.

As early as 1991, Mountziaris and Jensen¹ developed a kinetic model for the MOCVD deposition of GaAs from trimethylgallium and arsine. In their model, methyl radicals produced in the initial step were postulated to undergo hydrogen-abstraction reactions with TMGa or its decomposition byproducts, producing short-lived, highly reactive gallium methylene (GaCH₂). These reactive intermediates were proposed to play an important role in the deleterious incorporation of carbon in the growth process.

A thorough literature search shows that GaCH₂ has never been observed spectroscopically, either in the gas phase or in matrices and there are no computational studies available on the free radical. In fact, of the possible group III-methylene species BCH₂, AlCH₂, GaCH₂, InCH₂ and TlCH₂ only aluminum methylene, which we reported very recently,^{2,3} is now known. We used laser-induced fluorescence techniques to detect AlCH₂ among the decomposition products of trimethylaluminum in a pulsed electric discharge jet. The $\tilde{B}^2A_2 - \tilde{X}^2B_1$ band systems of AlCH₂ and AlCD₂, in the 513–483 nm region, were recorded and the 0-0 bands rotationally resolved which

afforded the molecular structures in both states. The observed "spin-splittings" were found to be predominantly caused by a large aluminum Fermi contact interaction in the excited state.

In the present work, we have succeeded in detecting the LIF spectra of GaCH_2 and GaCD_2 produced by the electric discharge degradation of trimethylgallium at the exit of a supersonic expansion into vacuum. The spectra have been assigned based on their similarity to those of aluminum methylene, on the predictable effects of deuteration and on the correspondence between the spectroscopically observed properties (electronic excitation energies, vibrational frequencies, deuterium isotope effects and rotational band contours) and those we calculate using high-level *ab initio* methods.

II. EXPERIMENT

The pulsed discharge jet technique, described in detail elsewhere,^{4,5} was used to produce rotationally cold gallium methylene free radicals in the gas phase. Moderately cold spectra (30-40 K) were obtained with the following conditions: Pyrophoric trimethylgallium (TMGa or TMGa-d_9) liquid was transferred in vacuum to a Pyrex U-tube held in a fume hood, cooled to -15 C (vapor pressure ~ 29 Torr) and pressurized with 40-50 psi of argon. The gas mixture was carried through stainless steel tubing from the fume hood to a pulsed molecular beam valve (General Valve, series 9) mounted in a vacuum chamber. The precursor gas pulses were expanded into a black Delrin flow channel where a pulsed electrical glow discharge between two stainless steel ring electrodes fragmented the trimethylgallium precursor, producing a variety of products. A 1.0 cm long, 5 mm ID cylindrical Delrin reheat tube⁶ added to the end of the discharge flow channel was found to increase production of Ga methylene radicals and to suppress the background glow from excited argon atoms. Much colder (8 -10K) spectra were obtained by diluting 15-30 Torr of trimethylgallium vapor with 500 psi of argon in a 1000 cm^3 stainless steel sample cylinder

(Swagelok 304L-HDF4-1000) and expanding the gas mixture at a pressure of 150-200 psi through the discharge and into vacuum.

Our initial searches for the gallium methylene radicals were conducted using the 2D LIF spectrometer, described in detail in a recent publication⁷, developed in the laboratory at Ideal Vacuum. This instrument uses a broadly tunable, high power optical parametric oscillator (Continuum Horizon OPO, 400–710 nm, linewidth 3–7 cm⁻¹, and energy 10–50 mJ/pulse) to produce low resolution LIF spectra and the corresponding emission spectrum at each laser step. In this fashion, wide ranges of the visible and UV regions can be surveyed with high sensitivity in an automated fashion, typically by scanning overnight.

Once promising LIF signals were found in the 2D LIF spectra, these were investigated more thoroughly using a higher resolution Lambda-Physik Scanmate 2E dye laser, operated at medium resolution (0.1 – 0.2 cm⁻¹ linewidth) or optionally at high resolution (0.035 cm⁻¹ linewidth) by inserting an intracavity etalon. The medium resolution LIF spectra were calibrated (+/- 0.1 cm⁻¹ or better) with optogalvanic signals from a neon-filled hollow cathode lamp.

Emission spectra were recorded by fixing the Scanmate dye laser on a prominent *Q*-branch in the LIF spectrum and dispersing the fluorescence with a Spex 500M monochromator. The emission signals were recorded with an intensified, gated CCD camera (Andor iStar 320T, wavelength range of photocathode 280–760 nm) mounted in the exit focal plane of the instrument. With suitable gating, scattered laser light was completely suppressed and resonance fluorescence down to the initially pumped level could be measured, along with red-shifted emission to higher vibronic levels of the lower state. The spectra were calibrated to an accuracy of 1 - 2 cm⁻¹ with argon emission lines from a Li/Ar hollow cathode lamp.

Trimethylgallium (Sigma-Aldrich) was used as received. TMGa-d₉ was synthesized by the high temperature reaction of deuterated iodomethane with gallium in the presence of magnesium according to the equation $6\text{CD}_3\text{I} + 3\text{Mg} + 2\text{Ga} \rightarrow 2(\text{CD}_3)_3\text{Ga} + 3\text{MgI}_2$ following the procedure of Zakharkin et al.⁸ A 150 cm³ stainless steel cylinder (Swagelok 304L-HDF4-150) was loaded with 1.44 g (21 mmol) of gallium metal chunks (Sigma-Aldrich), 0.93 g (38 mmol, slight excess) of magnesium powder (Sigma-Aldrich) and 8.97 g of CD₃I (62 mmol, Sigma-Aldrich, >99.5% D). The cylinder was sealed with a high-temperature bellows valve (Swagelok SS-4H2, threaded surfaces sealed with several layers of 3.5 mil Teflon tape), connected to a vacuum line and thoroughly degassed. After demounting from the vacuum line, the exit of the valve was further sealed with a threaded stainless-steel cap, and the vessel was heated in an oven at 170°C for 70 hours. After cooling, the contents were expanded into vacuum, purified by trap-to-trap distillation and analyzed by gas phase FTIR spectroscopy. This procedure gave 2.0 g (78% yield) of trimethylgallium-d₉ with a purity of better than 95%, as judged by comparison with published IR spectra.⁹

III. THEORETICAL CALCULATIONS

In previous theoretical work, we extensively explored the properties of the ground and several excited states of the isoelectronic AlCH₂ free radical², which provided a conceptual framework for the present, less far-reaching studies of gallium methylene. *Ab initio* calculations of the energies, geometries and vibrational frequencies of the ground and lowest two doublet and the first quartet electronic excited states of GaCH₂ and GaCD₂ were performed using the Molpro¹⁰ and CFOUR¹¹ quantum chemistry programs.

In Molpro, molecular orbitals were first obtained optimizing the ground and first two doublet excited electronic states in state averaged complete active space self-consistent field

(CASSCF)^{12,13} computations (9 electrons in 10 orbitals). Energies were then calculated by the internally contracted multireference configuration interaction (ICMRCI)^{14,15} method using the same active space as reference. The Davidson correction¹⁶, with relaxed reference¹⁷ was applied to the ICMRCI energies. In CFOUR, we started from Unrestricted Hartree Fock (UHF) orbitals, checked to avoid SCF spatial instabilities,¹⁸ followed by the coupled cluster singles and doubles with perturbative triple excitations¹⁹ (CCSD(T)) method for the ground state, and equations of motion methods [EOM-CCSD] for the electronic excited states.^{20,21} For both methods, the electron correlation treatment was either limited to valence electrons or extended to include the ten d-electrons of gallium.

For calculations with correlation treatment restricted to valence electrons, we used the aug-cc-pV(T+d)Z and aug-cc-pV(Q+d)Z²² bases for gallium and the aug-cc-pVTZ and aug-cc-pVQZ²³ bases for carbon and hydrogen. For calculations including d-electron correlation, we used the aug-cc-pwCVTZ^{24,25} bases for gallium and carbon and aug-cc-pVTZ for hydrogen.

In the first stages of this work, we explored the relative energies and stabilities of other isomers of GaCH₂. In Table I we report the geometries and frequencies of trans-HGaCH and CGaH₂, calculated with both CASSCF/ICMRCI and CCSD(T) methods. For trans-HGaCH, the results (geometry and frequencies) from the two methods are very similar. The situation is different for CGaH₂ of C_{2v} symmetry which was found to be a transition state at the ICMRCI level, with an imaginary in-plane asymmetric CGaH bending frequency, ω_6 . Removing the symmetry constraint, the structural optimization reverted to the trans-HGaCH geometry. Since the trans-HGaCH isomer is predicted to be 42.8 – 45.1 kcal/mol higher in energy and the CCSD(T) planar CGaH₂ species 97.0 kcal/mol above the GaCH₂ global minimum, it is unlikely that either of these isomers would be observed in our experiments.

The CASSCF/aug-cc-pVTZ state-averaged ground state molecular orbitals calculated at the ICMRCI/ aug-cc-pVTZ equilibrium geometry are shown in the Supplementary Material. The orbital occupations of the first three electronic states of GaCH₂ are the same as those of AlCH₂^{2,3}. The ground \tilde{X}^2B_1 state is well-described by the configuration:

$$(\text{core})(9a_1)^2(4b_2)^2(10a_1)^2(11a_1)^2(4b_1)^1$$

in which the unpaired electron in the highest occupied molecular orbital (HOMO) $4b_1$ is localized in an out-of-plane $2p$ orbital on the carbon atom. Promotion of an electron from the $11a_1$ orbital

PLEASE CITE THIS ARTICLE AS DOI: 10.1063/5.0182504

TABLE I. Ground state geometries, harmonic vibrational frequencies, and relative energies of the CGaH₂ and trans-HCGaH geometric isomers, calculated using Molpro at RHF/RCCSD(T) and CASSCF/ICMRCI levels of theory with the aug-cc-pV(T+d)Z basis.

	CASSCF/ICMRCI ^a	RHF/RCCSD(T)
trans-HCGaH $\tilde{X}^2A''(C_s)$		
$r(\text{GaC})/\text{\AA}$	1.8616	1.8668
$r(\text{GaH})/\text{\AA}$	1.5732	1.5747
$r(\text{CH})/\text{\AA}$	1.0916	1.0918
$\theta(\text{HGaC})/\text{deg}$	144.3	144.8
$\theta(\text{HCGa})/\text{deg}$	130.7	130.2
$\omega_1(\text{a}')/\text{cm}^{-1}$	3132.3	3136.3
$\omega_2(\text{a}')/\text{cm}^{-1}$	1942.3	1956.6
$\omega_3(\text{a}')/\text{cm}^{-1}$	750.3	757.6
$\omega_4(\text{a}')/\text{cm}^{-1}$	600.7	601.5
$\omega_5(\text{a}')/\text{cm}^{-1}$	393.7	386.9
$\omega_6(\text{a}'')/\text{cm}^{-1}$	445.4	430.0
$\Delta E(\text{kcal/mol})^b$	42.8	45.1
CGaH₂ $\tilde{X}^2B_1(C_{2v})$		
$r(\text{GaC})/\text{\AA}$	2.0377	2.0434
$r(\text{CH})/\text{\AA}$	1.5855	1.5861
$\theta(\text{HGaH})/\text{deg}$	123.0	123.1
$\omega_1(\text{a}_1)/\text{cm}^{-1}$	1926.2	1924.8
$\omega_2(\text{a}_1)/\text{cm}^{-1}$	636.8	703.1
$\omega_3(\text{a}_1)/\text{cm}^{-1}$	536.5	552.3
$\omega_4(\text{b}_1)/\text{cm}^{-1}$	444.5	508.9
$\omega_5(\text{b}_2)/\text{cm}^{-1}$	1922.4	1931.0
$\omega_6(\text{b}_2)/\text{cm}^{-1}$	20 <i>i</i> ^c	279.1
$\Delta E(\text{kcal/mol})^b$	95.4	97.0

^a CASSCF orbitals averaged for the three lowest doublet electronic states.

^b Relative to GaCH₂, calculated at the same level of theory.

^c The imaginary frequency indicates that for CGaH₂ the C_{2v} geometry is a saddle point at the CASSCF/ICMRCI level of theory. Lowering symmetry restrictions, geometry optimization leads to the trans-HCGaH isomer.

(primarily a lone pair $4s$ orbital on the gallium atom) to the HOMO gives rise to the low-lying \tilde{A}^2A_1 excited state with configuration

$$(\text{core})(9a_1)^2(4b_2)^2(10a_1)^2(11a_1)^1(4b_1)^2$$

Finally, promotion of an electron from the doubly occupied $11a_1$ orbital to the empty lowest unoccupied molecular $5b_2$ orbital (LUMO, π^* antibonding) produces the \tilde{B}^2A_2 state with dominant configuration

$$(\text{core})(9a_1)^2(4b_2)^2(10a_1)^2(11a_1)^1(4b_1)^1(5b_2)^1.$$

The structural and spectroscopic properties of the 2B_1 ground state of GaCH_2 , calculated both at ICMRCI and CCSD(T) levels, are collected in Table II. For both methods, we took the results obtained with the aug-cc-pVTZ basis as reference and tested their stability on increasing the size of the basis (aug-cc-pVQZ basis) and the effects of the inclusion the gallium d-electrons in the correlation treatment (aug-cc-pwCVTZ basis). The geometrical parameters obtained from the six combinations of method/basis agree within 0.04 \AA , 0.002 \AA and 0.3° for the Ga-C and C-H bond lengths and the H-C-H angle, respectively. As expected, the inclusion of d-electron correlation has its largest effect on the Ga-C bond length. The vibrational frequencies have only modest fluctuations as well, with the out-of-plane bending mode ω_4 showing the largest deviation (about 50 cm^{-1} for the H-isotopologue).

The 2A_1 first excited electronic state has been studied using the same combinations of method/basis and the results are tabulated in Table II. The agreement between the various approaches for the geometrical parameters $r(\text{GaC})$, $r(\text{CH})$ and $\theta(\text{HCH})$ is a bit looser, compared to the ground state, being 0.04 \AA , 0.004 \AA and 2° , respectively. Excluding ω_4 , the vibrational frequencies show general agreement within 51 cm^{-1} . In contrast, the out-of-plane mode, ω_4 , shows very large fluctuations, with frequencies around 1000 cm^{-1} for ICMRCI and ranging from about 1300 cm^{-1} to more than 2100 cm^{-1} for EOM-CCSD, with a clearly unphysical huge jump when the d-electron correlation is included. The source of such behavior is not clear.

Similar studies of the second excited electronic state, spanning the same combinations of methods and bases, are summarized in Table II. Initially, we assumed a planar C_{2v} structure with

PLEASE CITE THIS ARTICLE AS DOI: 10.1063/5.0182504

ω_1 (a ₁)/cm ⁻¹	3093.0/2233.4	3097.4/2236.8	3098.5/2237.5	3125.4/2256.6	3131.3/2260.9	3131.0/2260.1
ω_2 (a ₁)/cm ⁻¹	1347.8/997.9 [349.9]	1352.2/1002.2 [350.0]	1361.5/1009.5 [323.0]	1350.6/999.6 [351.0]	1352.7/1001.6 [351.1]	1350.2/998.8 [351.4]
ω_3 (a ₁)/cm ⁻¹	557.2/527.1 [30.1]	566.5/536.0 [30.5]	576.2/545.0 [30.5]	557.5/528.3 [29.2]	561.7/532.0 [29.7]	556.6/527.9 [28.7]
ω_4 (b ₁)/cm ⁻¹	242.5i/189.5i	221.2i/172.7i	271.8i/212.3i	695.0/542.5 [152.5]	700.0/546.4 [153.6]	762.5/595.4 [167.1]
ω_5 (b ₂)/cm ⁻¹	3206.4/2387.9	3213.8/2393.6	3214.5/2394.6	3240.8/2414.2	3250.0/2421.1	3251.8/2424.4
ω_6 (b ₂)/cm ⁻¹	704.4/528.1 [176.4]	710.9/533.1 [177.8]	724.5/543.5 [181.0]	697.5/522.7 [174.8]	702.2/526.2 [176.0]	714.4/535.5 [178.9]
T_0 /cm ⁻¹	<i>a</i>	<i>a</i>	<i>a</i>	21017/20929 [88]	21258/21171 [88]	24276/24177 [99]
\tilde{B}^2A'' (Nonplanar)						
$r(\text{GaC})/\text{\AA}$	2.0015	1.9951	1.9710			
$r(\text{CH})/\text{\AA}$	1.0886	1.0874	1.0874			
$\theta(\text{HCH})/\text{deg}$	115.1	115.0	115.2			
ϕ/deg^b	24.0	24.0	24.1			
$\text{barrier}/\text{cm}^{-1} \text{ }^c$	159	32	75			
ω_1 (a ₁)/cm ⁻¹	3074.2/2221.0	3078.7/2224.4	3080.5/2225.6			
ω_2 (a ₁)/cm ⁻¹	1352.2/1002.7 [349.5]	1354.5/1005.0 [349.5]	1367.7/1015.1 [352.6]			
ω_3 (a ₁)/cm ⁻¹	543.9/509.6 [34.3]	551.6/516.8 [34.8]	561.7/526.3 [35.4]			
ω_4 (b ₁)/cm ⁻¹	334.6/262.8 [71.8]	341.4/268.0 [73.4]	337.3/264.7 [72.6]			
ω_5 (b ₂)/cm ⁻¹	3181.2/2367.0	3188.1/2372.1	3188.6/2372.8			
ω_6 (b ₂)/cm ⁻¹	719.5/536.6 [182.9]	722.6/539.2 [183.4]	740.3/552.5 [187.8]			
T_0 /cm ⁻¹	20668/20622 [46]	20791/20746 [45]	21551/21500 [51]			
\tilde{a}^4A_2						
$r(\text{GaC})/\text{\AA}$	1.9971	1.9905				
$r(\text{CH})/\text{\AA}$	1.0861	1.0849				
$\theta(\text{HCH})/\text{deg}$	121.5	121.5				
μ/debye	-0.775	-0.785				
ω_1 (a ₁)/cm ⁻¹	3098.7/2237.1	3104.8/2241.7				
ω_2 (a ₁)/cm ⁻¹	1341.3/ 992.2	1356.2/1004.3				
ω_3 (a ₁)/cm ⁻¹	540.9/ 512.1	558.6/528.3				
ω_4 (b ₁)/cm ⁻¹	681.4/ 531.9	693.8/541.7				
ω_5 (b ₂)/cm ⁻¹	3212.5/ 2392.8	3220.1/2398.7				
ω_6 (b ₂)/cm ⁻¹	683.9/ 512.7	693.8/ 526.4				
T_0 /cm ⁻¹	18344/18262	18878/18789				

^a T_0 not calculated.^b Ga atom out of the HCH plane angle.

^c Energy barrier to C_{2v} geometry.

term symbol \tilde{B}^2A_2 . The geometric parameters obtained with this constraint are very similar, with $r(\text{GaC})$, $r(\text{CH})$ and $\theta(\text{HCH})$ differences within 0.04 Å, 0.004 Å and 0.8°, respectively. Moreover, all the vibrational frequencies, excluding ω_4 , agree within 46 cm^{-1} . At the ICMRCI level, the ω_4 frequency is always imaginary, indicating that the imposed C_{2v} symmetry corresponds to a transition state. Only small differences are observed on changing the basis set. Conversely, at the EOM-CCSD level, the ω_4 frequency is definitely positive, with calculated frequencies around 700 cm^{-1} . As we shall see, such high values are clearly unreliable, as they do not have any correspondence with experiment (*vide infra*), but nevertheless they are reported for completeness.

The question is: why are the ICMRCI and EOM-CCSD results so different for the ω_4 mode? An important clue comes from an examination of the spin expectation values in the CFOUR EOM-CCSD wavefunctions of the excited states. We restrict our discussion to the results from the aug-cc-pVTZ basis as the outcomes from other bases are very similar. For the \tilde{A}^2A_1 state, the expectation value S^2 calculated by CFOUR at the equilibrium geometry is 0.80, which is fairly close to the theoretical value for a pure doublet of 0.75. The situation is very different for the second excited state with CFOUR giving $S^2 = 2.91$, which is closer to the 3.75 expectation value of a pure quartet state. Clearly, the EOM-CCSD wavefunction of the second excited state is strongly spin contaminated, casting doubt on the calculated properties.

On the other hand, the results from Molpro do not suffer from spin contamination, since the CASSCF and ICMRCI method is based on Configuration State Functions (CSF) which are eigenfunctions of both S^2 and S_z [see for example ref. 26]. On lowering the C_{2v} symmetry constraint in the calculation of the second excited state, the ICMRCI method finds a bent structure with small out-of-plane angle ($\approx 24^\circ$) and very small barrier to planarity (159 cm^{-1} with the aug-cc-pVTZ basis). It turns out that the ICMRCI calculated ω_4 frequency, its H/D isotopic shift and the computed T_0 isotope shift are all in reasonable accord with experiment (*vide infra*), suggesting that they are the most reliable.

In summary, ICMRCI computations point to a slightly nonplanar structure for the second excited state. However, this finding is in conflict with experiment, since no single quanta transitions of ω_4 are observed. It can be argued that, in the presence of a barrier to planarity much lower than the vibrational zero-point energy, the molecule may behave as if it is effectively planar. Most probably, the recovered nonplanar structure is due to the limitations, both intrinsic and practical, of the ICMRCI method we used. In fact, we observed (see Table II) that the barrier tends

to decrease either by increasing the basis size or by extending the correlation treatment to include gallium d-electrons, suggesting that a planar structure may be achieved by increasing both simultaneously.

Another pitfall of our treatment may be the neglect of spin-orbit interactions with neighboring quartet states. Indeed, the first quartet state of GaCH₂ (\tilde{a}^4A_2 , see Table II) lies only ~ 2500 cm⁻¹ below the second excited doublet state. At planar C_{2v} geometries, no spin-orbit interaction between the \tilde{B}^2A_2 and \tilde{a}^4A_2 states can take place. However, for C_s non-planar geometries, a bending-dependent nonzero doublet-quartet spin-orbit interaction can occur through the LS_i component of the spin-orbit operator,²⁷ where i is the axis perpendicular to the symmetry plane of the molecule. The energy of the quartet state increases quickly upon bending (the ω_4 frequency of the \tilde{a}^4A_2 state is ~ 700 cm⁻¹, see Table II) as well as the extent of the interaction between the two states, resulting in a “push-up” effect on the out-of-plane bending potential of the \tilde{B}^2A_2 state when spin-orbit interaction is included. In short, we speculate that the slight non-planarity of the second excited state at the ICMRCI level is an artifact originating from a synergic effect of the many inherent approximations made in the calculation.

IV. RESULTS AND ANALYSIS

A. 2D LIF survey spectra

Fig. 1 shows a small portion of the 2D LIF spectrum obtained from the products of a discharge through TMGa vapor. The top panel shows the total LIF signal, and the bottom panel shows the color-coded emission spectrum obtained at each laser wavenumber. The emission spectra are displayed vertically as displacement (in cm⁻¹) from the laser (laser wavenumber – emission wavenumber) which gives a direct measure of the lower state energy of each transition. The spectra show a series of three bands in the 22 200 – 23 700 cm⁻¹ region that all have similar rotational contours and similar emission spectra, very reminiscent of the 2D LIF spectrum of AlCH₂.³ The emission spectra show prominent intervals of 515 and 1340 cm⁻¹, which can be

readily ascribed to the ν_3'' (Ga-C stretch) and ν_2'' (CH₂ scissors) vibrations (Table II) of GaCH₂, respectively. If the first LIF feature is assigned as the 0-0 band, then the maximum at 22 230 cm⁻¹ compares favorably to the calculated T_0 of 21 551 cm⁻¹ (nonplanar, aug-cc-pwCVTZ, d-electrons correlated Table II) for GaCH₂. The 2D LIF spectrum is complicated by fluorescence from other impurity molecules formed in the discharge, particularly at energies above 23 000 cm⁻¹. Nevertheless, all indications are that the three bands identified in the 2D LIF spectrum are due to the previously unidentified gallium methylene free radical.

B. 0-0 band LIF spectra and confirmation of the gallium methylene assignment

Medium resolution LIF spectra of the 0-0 bands of GaCH₂ and GaCD₂ at two different rotational temperatures are shown in Fig. 2, along with calculated band contours based on the rotational constants obtained from the ground and excited state *ab initio* molecular geometries. The rotational structure was computed using the PGOPHER program,²⁸ assuming a linewidth of 0.4 cm⁻¹, neglecting unpaired electron spin-rotation and gallium atom hyperfine effects, which are not resolved in our spectra, and including only the ⁶⁹Ga isotopologue in each case. For GaCH₂ with a ²B₁ ground state, nuclear statistical weights favor even K_a values by a factor of 3, whereas in GaCD₂, odd K_a values have twice as many nuclear spin states as even values. These expectations are robustly borne out in the GaCH₂ spectrum in Fig. 2, with a strong central rQ_0 branch flanked by weaker pQ_1 and rQ_1 branches. In GaCD₂, the situation is reversed, with a weak central Q branch and stronger $K_a''=1$ Q branches on either side, precisely as expected. Furthermore, the separation of the Q branches is consistent with the calculated molecular structures and the lack of resolved rotational structure is indicative of overlapping spectra from the ⁶⁹Ga (60.1 %) and ⁷¹Ga (39.9 %) isotopologues in

This is the author's peer reviewed, accepted manuscript. However, the online version of record will be different from this version once it has been copyedited and typeset.

PLEASE CITE THIS ARTICLE AS DOI: 10.1063/5.0182504

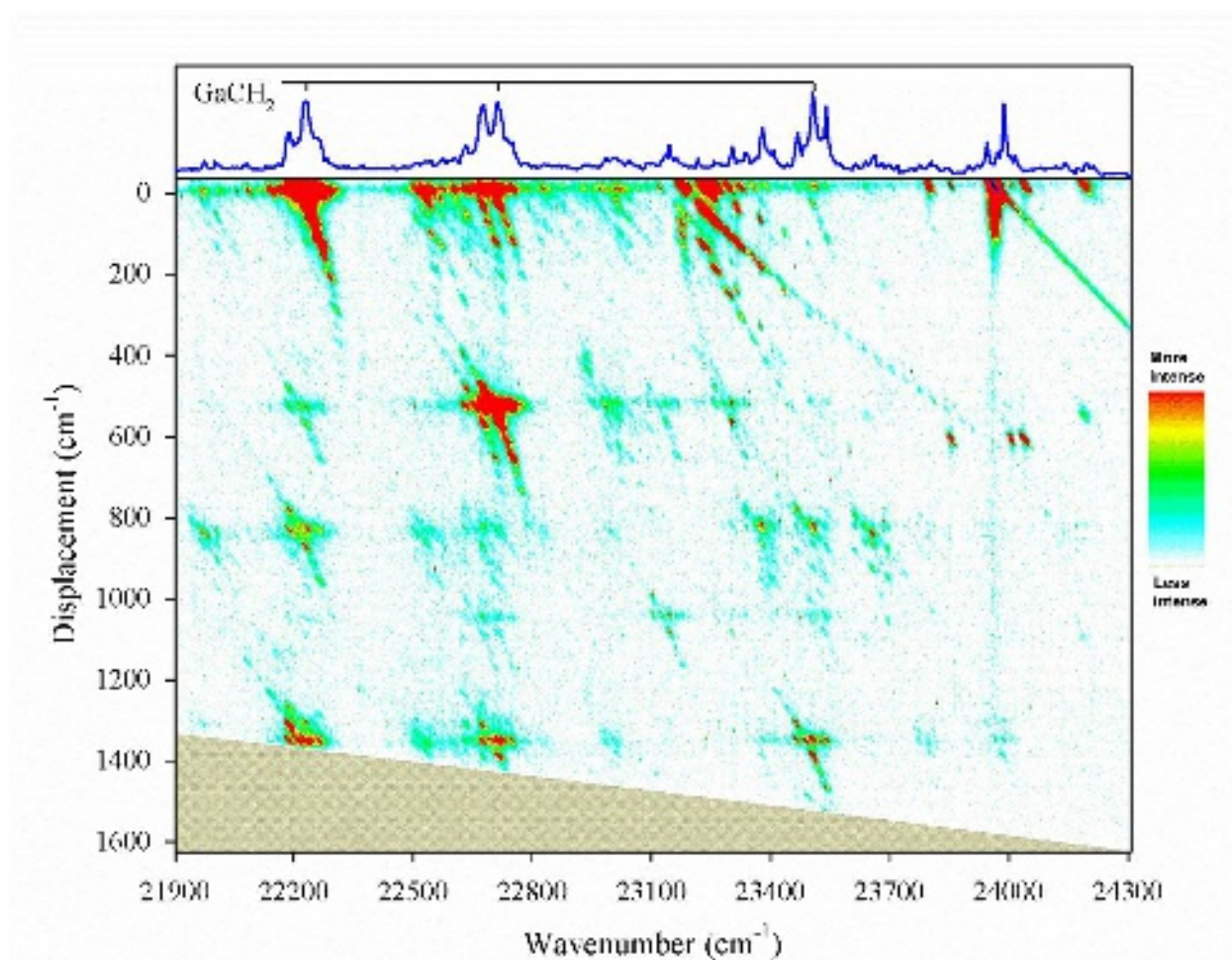


FIG. 1. A segment of the 2D LIF spectrum of the products of an electric discharge through a mixture of trimethylgallium vapor and high-pressure argon. The horizontal axis is the excitation laser wavenumber (cm^{-1}). The top spectrum is the total LIF fluorescence, and the bottom panel shows the emission spectrum obtained at each excitation laser wavenumber. The emission spectra are arranged vertically and are plotted as displacement in cm^{-1} from the laser wavenumber.

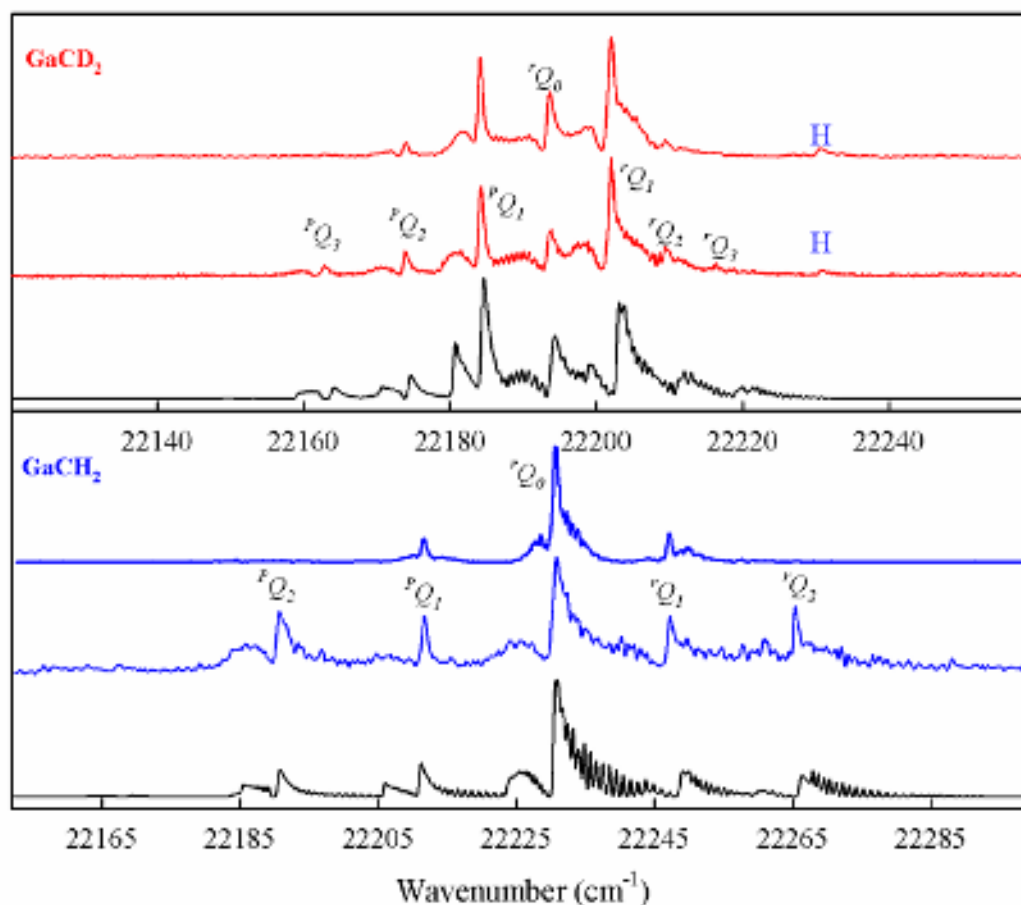


FIG. 2. Low resolution LIF spectra of the 0-0 bands of GaCD₂ (top) and GaCH₂ (bottom). In each case, the top trace is the spectrum obtained at a rotational temperature of 8-10 K, the middle trace was obtained under milder expansion conditions (30-40 K) and the bottom trace is the spectrum calculated from the planar IC-MRCI (aug-cc-pwCVTZ d-electrons correlated) *ab initio* molecular structures in Table II. The letter H denotes GaCH₂ impurity features in the GaCD₂ spectra.

natural abundance. By fitting the observed Q -branch wavenumbers of the 30 K 0-0 bands (Fig. 2) to

$$\bar{\nu}(Q) = T_{00} + (A - \bar{B})'(K'_a)^2 - (A - \bar{B})''(K''_a)^2 \quad (1)$$

we obtained approximate values for the band origin and $(A - \bar{B}) \approx A$ values of the upper and lower states, yielding GaCH₂: $(A - \bar{B})'' = 10.010 \pm 0.036$, $(A - \bar{B})' = 9.332 \pm 0.018$ and GaCD₂: $(A - \bar{B})'' = 4.870 \pm 0.009$ and $(A - \bar{B})' = 4.418 \pm 0.009$ cm⁻¹. The calculated H/D 0-0 band isotope shift of 45-51 cm⁻¹ (Table II) is also in good accord with the experimental value of 32.4 cm⁻¹ derived from the fitted band origins.

We attempted to record high-resolution LIF spectra of the 0-0 band of GaCH₂, as shown in Fig. 3. The $K'_a = 1 - K''_a = 0$ P - and R -branches clearly show the splittings expected for a molecule in a doublet state, further confirming the spectrum as due to the gallium methylene free radical. Unfortunately, due to the presence of the two gallium isotopes in natural abundance, the crucial asymmetry-split branches (rR_1 , rP_1 , pR_2 and pP_2) were not resolvable at our highest resolution (0.035 cm⁻¹) so a detailed rotational analysis and experimental determination of the molecular structure was not possible in the present investigation. We defer discussion of the vibronic assignments of the vibrationally resolved LIF spectra until after the analysis of the emission spectra.

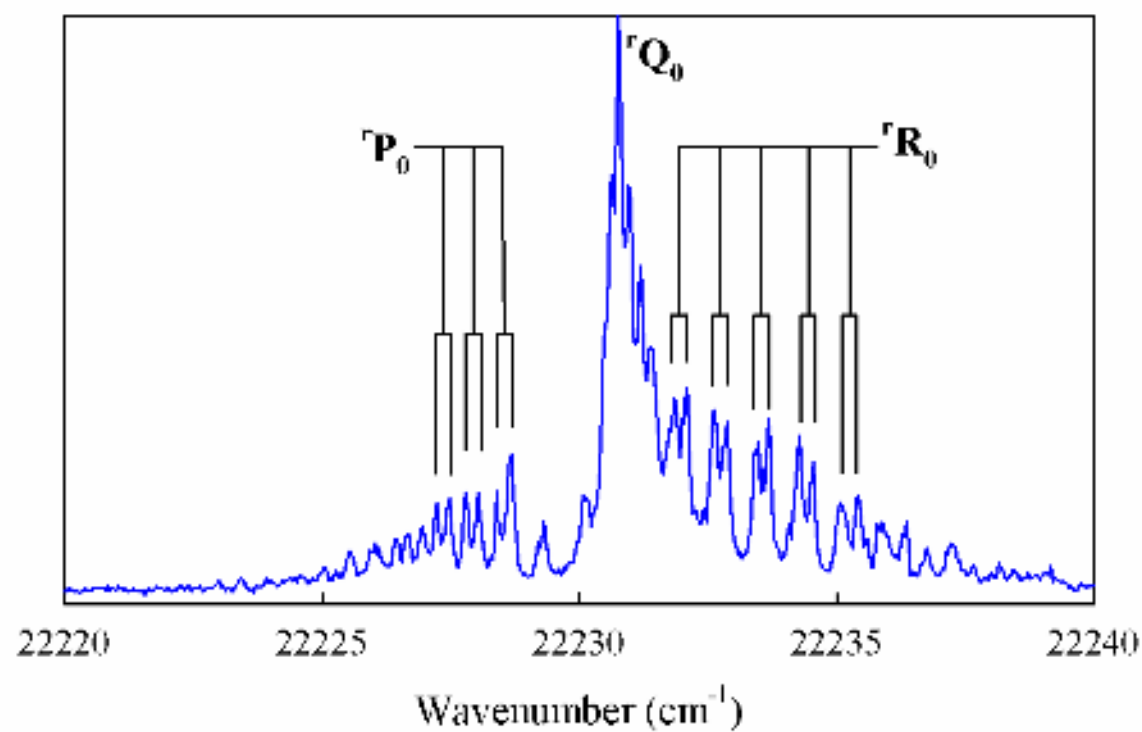


FIG. 3. A high resolution LIF spectrum of the central portion of the 0-0 band of GaCH₂ showing resolved spin-splittings.

C. Emission spectra and the vibrational energy levels of the ground state

1. 0-0 band emission spectra and selection rules

The 0-0 band emission spectra of GaCH₂ and GaCD₂ are compared in Fig. 4, plotted as displacement from the laser excitation wavenumber, giving a direct measure of the ground state energy of each transition. We have also recorded extensive emission spectra from the various other LIF bands of both isotopologues and these are reported in the Supplementary Information. Since the LIF spectra show resolved rotational subbands, laser excitation of different branches gives somewhat different emission spectra. As shown in Fig. 4, ^pQ₁ excitation gives a single $K'_a = 0 - K''_a = 1$ transition down to each lower state vibronic level. Due to the nuclear statistical weights and rotational cooling in the free jet expansion, these branches are intense in GaCD₂ but relatively weak in GaCH₂ (see Fig. 2). For comparison, we show in Fig. 4 the corresponding spectra obtained by GaCH₂ ^rQ₀ excitation, which gives two branches ($K'_a = 1$ down to $K''_a = 0$ and 2) with an approximate spacing of 4A'' and GaCD₂ ^rQ₁ excitation (to $K''_a = 1$ and 3 with splitting ≈ 8 A'').

The vibronic selection rules mandate unrestricted quantum number changes for the totally symmetric vibrational modes ($\nu_1 - \nu_3$) of planar GaCH₂. Although transitions to even quanta (4₂, 6₂ etc.) of the non-totally symmetric modes are formally allowed, they are expected to be very weak unless the vibrational frequency changes substantially on electronic excitation, as is likely the case (Table II) for modes 4 and 6. In addition, vibronically induced bands may occur in the spectrum. The transition moment integral, with operator **M**, including vibronic interaction is

$$R_{e'v'e''v''} = \int \Psi_{ev}^{\prime*} \mathbf{M} \Psi_{ev}'' d\tau \quad (2)$$

This is the author's peer reviewed, accepted manuscript. However, the online version of record will be different from this version once it has been copyedited and typeset.

PLEASE CITE THIS ARTICLE AS DOI: 10.1063/5.0182504

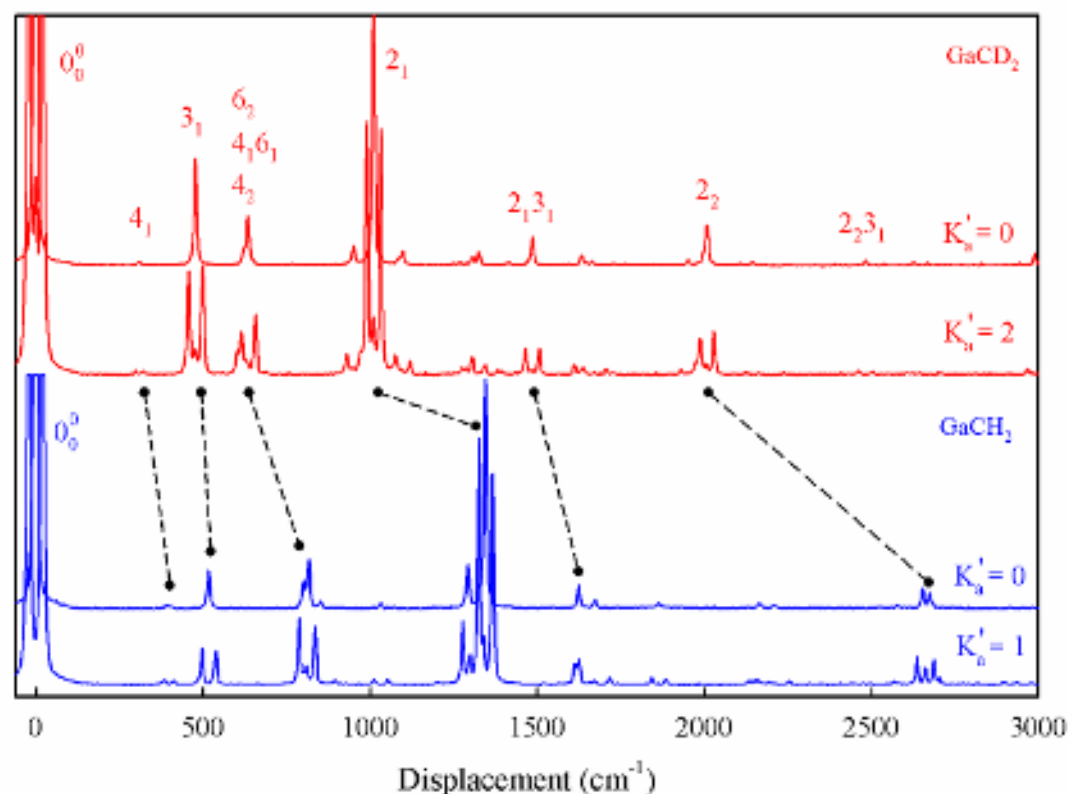


FIG. 4. The 0-0 band emission spectra of GaCD₂ (top) and GaCH₂ (bottom). For GaCD₂, the upper trace is emission from $K'_a = 0$ (pQ_1 excitation) and the lower trace is emission from $K'_a = 2$ (rQ_1 excitation). For GaCH₂, the upper trace is emission from $K'_a = 0$ (pQ_1 excitation) and the lower trace is emission from $K'_a = 1$ (rQ_0 excitation). Features with the same lower state vibrational assignments are linked by dashed lines.

which, for a b_2 GaCH₂ vibration (ν_5 and ν_6), can only be nonzero for a transition moment along the a -axis (C_2 axis) such that $A_2 \times B_1 \times b_2 = A_1$. Thus, the 6_1^0 parallel band can be vibronically induced by borrowing intensity from an allowed $B_1 \leftarrow B_1$ electronic transition. In direct contrast, for the ν_4 vibration of b_1 symmetry, the product of the vibronic symmetries is $A_2 \times B_1 \times b_1 = A_2$ and there is no transition moment of A_2 symmetry in C_{2v} so the 4_1^0 band cannot be vibronically induced. Finally, for a combination band such as $4_1^0 6_1^0$, the direct product is $A_2 \times B_1 \times b_1 \times b_2 = B_1$ which is allowed for a transition involving c -type rotational selection rules. In summary, vibronically induced transitions involving odd quantum number changes in the b_2 modes can occur as parallel bands and those involving odd combinations of $b_1 + b_2$ modes will appear as perpendicular bands indistinguishable at modest resolution from the allowed b -type bands in the spectrum.

If GaCH₂ is slightly nonplanar (C_s symmetry) in the excited state, as predicted by our IC-MRCI calculations, then $\nu_1 - \nu_4$ are all of a' symmetry and unrestricted quantum number changes in these modes are allowed, giving rise to perpendicular bands. The greater the nonplanar distortion, the greater the expected Franck-Condon activity in the ν_4 out-of-plane bending mode. Although rigorously forbidden in C_{2v} symmetry, the 4_1^0 band would be expected to gain intensity in proportion to the extent of nonplanarity.

Before assigning the emission spectra, it is also necessary to consider the rovibronic structure of the observed bands in more detail, as illustrated in Fig. 5. The spectra are complicated by the observation of resolved subbands and the near degeneracy of ν_4'' and ν_6'' . What we measure is the displacement of each band from the excitation laser wavenumber which gives a direct measure of the ground state vibrational energy. As shown on the LHS of Fig. 5, pQ_1 excitation

gives a displacement \mathbf{D}_1 (laser wavenumber – transition wavenumber) which measures the interval between $K_a = 1$ of the ground state vibrational level of interest (3_1 in the Fig.) and $K_a = 1$ of the zero-point level whereas rQ_0 excitation gives a more direct measure \mathbf{D}_2 of the $K_a = 0$ separation. As long as the $(A - \overline{B})$ values are comparable in the two ground state vibrational levels, as they usually are, $\mathbf{D}_1 = \mathbf{D}_2$ within the $\pm 1 \text{ cm}^{-1}$ accuracy of the emission measurement. For example, we measure 3_1 to have a vibrational energy of 516.6 cm^{-1} from both 0-0 band pQ_1 and rQ_0 emission spectra. Since pQ_1 excitation results in single $K'_a = 0 - K''_a = 1$ transitions, with many fewer overlapping lines, we usually choose such spectra for displacement measurements.

In the case of vibronically induced bands, such as 6_1^0 , the emission bands obey a -type ($\Delta K_a = 0$) selection rules and, in the absence of perturbations, one would expect all the Q -branch transitions to be coincident. However, 6_1 is very likely perturbed by the 4_1 level just below it as shown in the middle of Fig. 5. The product of the 6_1 and 4_1 vibrational symmetries is $b_2 \times b_1 = A_2$, which mandates an a -axis Coriolis interaction with matrix element $\xi_{46}^a K_a$. This would not affect the 6_1 $K_a = 0$ levels, but $K_a = 1, 2$ would be progressively displaced upward, as illustrated. In this case, the pQ_1 displacement \mathbf{D}_3 needs to be corrected by adding the ground state $(A - \overline{B})$ value, whereas the rQ_0 displacement \mathbf{D}_4 is larger than necessary by the 6_1 $K_a = 1 - K_a = 0$ interval.

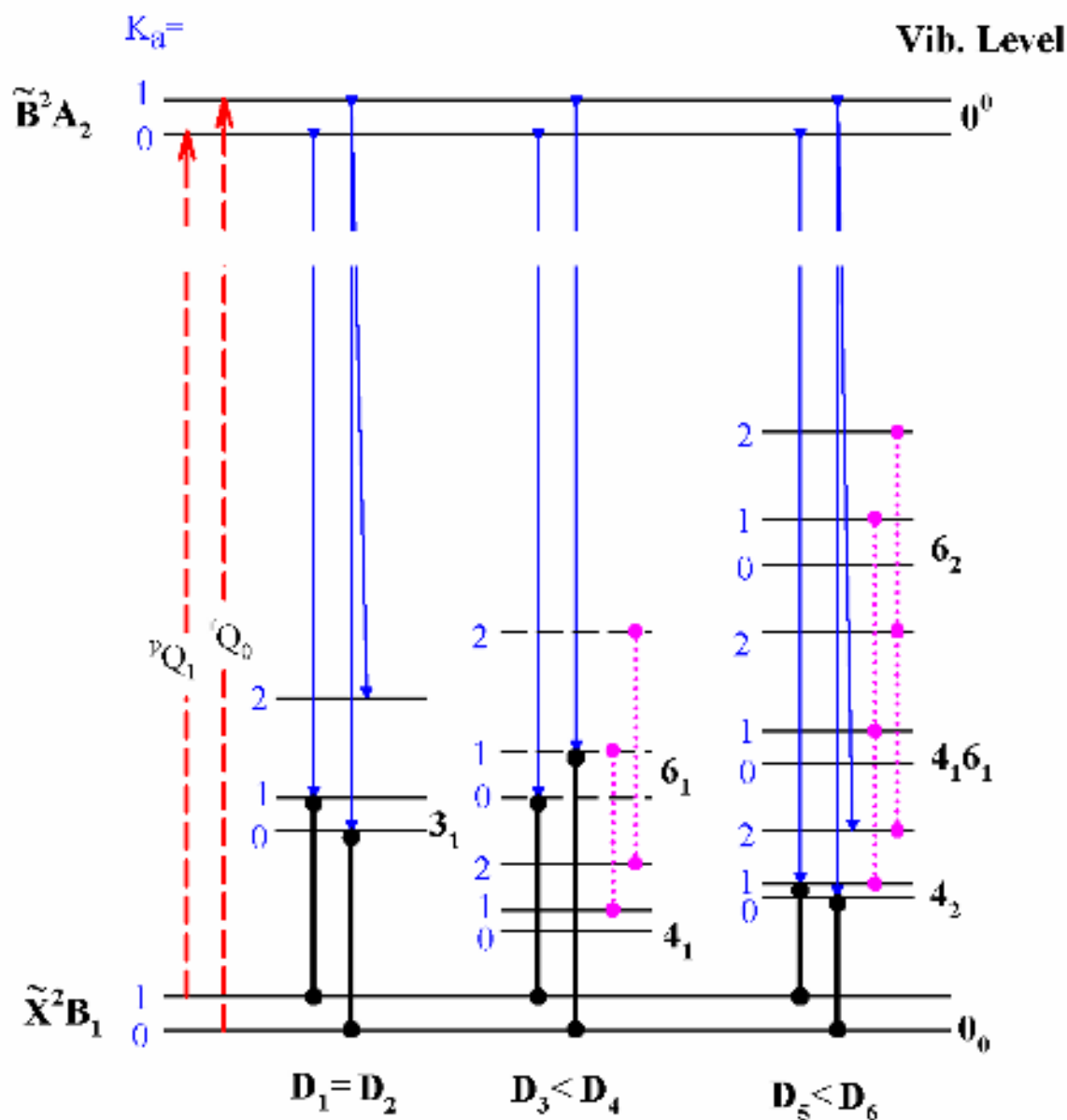


FIG. 5. Schematic energy level diagram showing the intervals that define the measured emission displacements (D_1 , D_2 etc.) subsequent to laser excitation of the pQ_1 and rQ_0 rotational branches of the 0-0 band of gallium methylene. The dotted lines denote Coriolis interactions between adjacent vibrational levels. The dashed lines indicate pQ_1 and rQ_0 laser excitation transitions.

Finally, we consider emission transitions down to the 4_2 , 4_16_1 and 6_2 triad of levels, which appear in many of the spectra. In this case, all the transitions involve $\Delta K_a = \pm 1$, but there are Coriolis complications, with $\Delta K_a = 0$ a -axis interactions possible between 4_2 and 4_16_1 and between 4_16_1 and 6_2 . These would have the effect of compressing the K stacks in 4_2 , inflating them in 6_2 and conceivably leaving them largely unchanged in 4_16_1 , as illustrated in Fig. 5. For emission down to 4_2 , the pQ_1 displacement \mathbf{D}_5 is then less than the true vibrational interval \mathbf{D}_6 . The energy level diagram indicates that the pQ_1 displacement $\approx {}^rQ_0$ displacement for 4_16_1 , and the 6_2 emission is the opposite of 4_2 (pQ_1 displacement $> {}^rQ_0$ displacement). In all cases, the rQ_0 displacement gives the correct vibrational interval, whereas the 4_2 and 6_2 pQ_1 displacements have to be corrected for Coriolis effects.

2. Vibrational assignments

For brevity in our discussion of the analysis of the emission spectra, comparisons of the vibrational frequencies will subsequently be denoted as GaCH₂/GaCD₂ and, except where noted, all quoted *ab initio* values refer to the IC-MRCI aug-cc-pwCVTZ, d-electrons correlated results from Table II. The resonance fluorescence down to the zero-point level dominates the 0-0 band spectra (Fig. 4), consistent with *ab initio* predictions that the molecular structure changes little on electronic excitation. The second most intense feature is readily assigned as the transition to $\nu_2'' = 1347/1011 \text{ cm}^{-1}$ (*ab initio* = 1384/1035 cm^{-1}). The 2_n progression can be readily followed out to 3 quanta in GaCH₂ and 5 quanta in the various emission spectra of GaCD₂. The next prominent feature occurs at 517/478 cm^{-1} (*ab initio* = 533/498 cm^{-1}) and the lack of a substantial deuterium isotope effect identifies it as ν_3'' (Ga-C stretch) which can be followed in various spectra out to 3_5 in both isotopologues. Other prominent features in the emission spectra are readily identified as

transitions down to combinations of ν_2 and ν_3 . The ν_1'' frequency is predicted to be very high (*ab initio* = 3037/2202 cm^{-1}) and has not been positively identified in any of our spectra.

The 0-0 band emission spectra exhibit very weak rQ_0 excitation features at 404/316 cm^{-1} and overlapping clusters of bands in the 800-852/622-648 cm^{-1} regions, all of which must involve the low-frequency, non-totally symmetric modes ν_4 and ν_6 . The 404/316 cm^{-1} intervals can only be assigned as single quanta, which must be either the 4_1^0 (*ab initio* = 400/313 cm^{-1}) perpendicular transitions or the vibronically induced 6_1^0 (*ab initio* = 419/316) parallel transitions. Since experimentally pQ_1 excitation gives single features and rQ_0 excitation gives doublets, we assign the 404/316 cm^{-1} features as the 4_1^0 bands which gain intensity due to the slight nonplanarity of the excited state. The 4_1^0 rQ_0 splittings are anomalously small (19/8 cm^{-1} compared to 42.2/20.5 cm^{-1} for the 3_1^0 emission bands), which we hypothesize must be due to ν_4 : ν_6 Coriolis coupling, much as occurs in formaldehyde.²⁹ Thus, if 6_1 is slightly above 4_1 , the *a*-axis Coriolis interaction does not perturb the $K_a = 0$ levels but the $K_a = 1$ levels repel each other, accounting for the small 4_1 splitting (see Fig. 5).

Building on the ν_6 identification, GaCH_2 rQ_0 features at 808 (2×404), 855 (2×427.5) and 831 ($404 + 427$) cm^{-1} can then be readily assigned to the levels 4_2 , 6_2 and 4_16_1 . Similar GaCD_2 rQ_0 features were found at 629 (2×314.5) [4_2], 655 (2×327.5) [6_2] and 642 ($314.5 + 327.5$) [4_16_1] cm^{-1} . These energy levels are shown schematically on the RHS of Fig. 5.

The 6_2^0 bands derive their intensity from the substantial difference in the ν_6 frequencies in the combining electronic states. Using the harmonic oscillator approximation, an expression for the 6_2^0 to 0_0^0 band intensity ratio can be derived as³⁰

$$\frac{I(6_2^0)}{I(0_0^0)} = \frac{1}{2} \frac{\bar{\nu}^3(6_2^0)}{\bar{\nu}^3(0_0^0)} \left[\frac{\omega'_6 - \omega''_6}{\omega'_6 + \omega''_6} \right]^2 \quad (3)$$

where the $\bar{\nu}$ symbols are the vibronic transition frequencies (cm^{-1}) and the ω 's are the vibrational frequencies in the two states. Using GaCH_2 *ab initio* frequencies of $\omega'_6 = 740.3$ and $\omega''_6 = 419.3$ cm^{-1} (Table II) gives a ratio of 0.034, about a factor of 5 larger than the experimental value of 0.006. Further combinations and overtones of these intervals can be found throughout the spectra.

Fig. 6 shows a comparison of the emission spectra from two of the weaker, higher wavenumber LIF bands, one of GaCD_2 ($^pQ_1 = 23\,570.8$ cm^{-1}) and one of GaCH_2 ($^pQ_1 = 23\,363.2$ cm^{-1}). These spectra differ dramatically from those of the 0-0 bands (Fig. 4), with very weak fluorescence down to 0_0 , 3_1 and 2_1 but very prominent transitions to the 4_2 , 4_16_1 and 6_2 triplet of levels. In addition, the GaCD_2 overtones 4_4 , 4_36_1 and 6_4 are also readily identified. In addition, some of the emission spectra of GaCD_2 (see Supplementary Information) exhibit strong transitions down to levels at 1313 and 1333 cm^{-1} in the ground state. The only viable assignments on energetic grounds are 2_14_1 and 2_16_1 , respectively, although such bands would normally be expected to be very weak.

Although the emission spectra extend to displacements of 3 000 – 4 000 cm^{-1} , in many cases assignments of the less prominent bands above 1 500 cm^{-1} proved quite difficult, due to Coriolis coupling, Fermi resonances, overlap and multiple possible quantum number

This is the author's peer reviewed, accepted manuscript. However, the online version of record will be different from this version once it has been copyedited and typeset.

PLEASE CITE THIS ARTICLE AS DOI: 10.1063/5.0182504

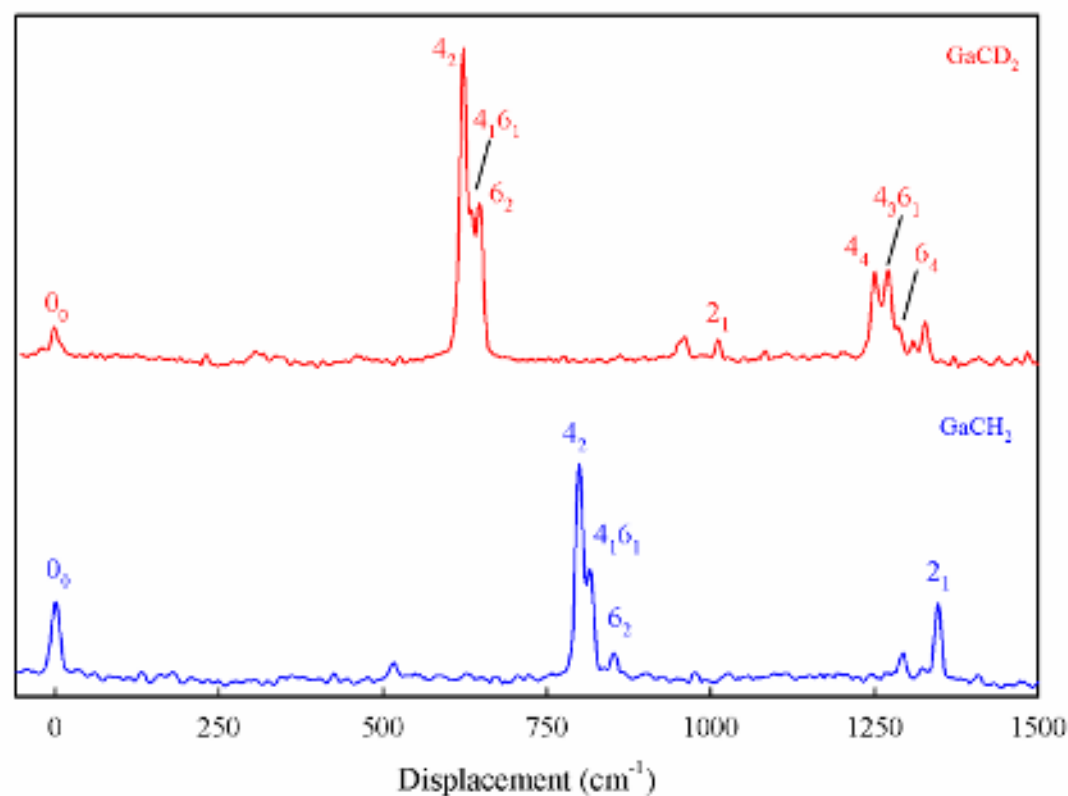


FIG. 6. Portions of the emission spectra of GaCD₂ (top, pQ_1 branch at 23570.8 cm⁻¹) and GaCH₂ (bottom, pQ_1 branch at 23363.2 cm⁻¹) that show strong transitions down to levels involving ν_4'' and ν_6'' .

combinations. It also proved impossible to differentiate between the 4_36_1 and 4_16_3 levels, which are nearly degenerate, so we have simply assigned them as the former. We present in Table III the measured ground state vibrational energy levels of both isotopologues along with our best attempts at assignments.

Although the $\tilde{A}^2A_1 - \tilde{X}^2B_1$ electronic transition is orbitally forbidden, we speculated that the emission from the upper state might be observable as a series of weak vibronically induced bands, which would pinpoint the location of the \tilde{A} state. For this purpose, we fixed the laser on the intense 1Q_0 branch of GaCH_2 and stepped our monochromator in overlapping segments from 550 – 850 nm, recording any emission with our gated CCD detector. No GaCH_2 fluorescence was observed.

D. Analysis of the LIF spectra

Fig. 7 shows the complete LIF spectra of GaCH_2 and GaCD_2 , recorded at a rotational temperature of 8-10 K. Above $22\,800\text{ cm}^{-1}$ the spectra were overlapped by impurity bands (GaH , GaD , CH , CD etc.) with fluorescence lifetimes much shorter than the $\sim 2 - 4\text{ }\mu\text{s}$ decays of gallium methylene. We have used temporal gating to eliminate these strong impurity bands from the spectra in Fig. 7. In addition, we recorded emission spectra from all the bands that had the appropriate gallium methylene fluorescence lifetime and rotational contour as an aid to making upper state assignments. We note that the emission spectra were useful when there were overlapping bands (cf. particularly $23\,400 - 23\,600\text{ cm}^{-1}$ of GaCD_2 LIF) as the number of peaks

TABLE III. Summary of the ground state vibrational levels of GaCH₂ and GaCD₂ measured from single vibronic level emission spectra.

GaCH ₂			GaCD ₂		
Energy (cm ⁻¹)	Assignment	Comment	Energy (cm ⁻¹)	Assignment	Comment
404	4 ₁	v ₆ = 404	314	4 ₁	v ₄ = 314
517	3 ₁	v ₃ = 517	478	3 ₁	v ₃ = 478
808	4 ₂	404+404	622	4 ₂	4 ₁ + 308
831	4 ₁ 6 ₁	4 ₁ + 427	634	4 ₁ 6 ₁	4 ₁ + 320
855	6 ₂	v ₆ = 428	648	6 ₂	v ₆ = 324
1032	3 ₂	3 ₁ + 515	951	3 ₂	3 ₁ + 473
1298	3 ₁ 4 ₂	3 ₁ + 781	1011	2 ₁	v ₂ = 1011
1318	3 ₁ 4 ₁ 6 ₁	3 ₁ + 801	1092	3 ₁ 4 ₂	3 ₁ + 614
1347	2 ₁	v ₂ =1347	1107	3 ₁ 4 ₁ 6 ₁	3 ₁ + 629
1542	3 ₃	3 ₂ + 510	1118	3 ₁ 6 ₂	3 ₁ + 640
1632	4 ₄	4 ₂ + 824	1255	4 ₄	4 ₂ + 633
1647	4 ₃ 6 ₁	4 ₁ 6 ₁ + 816	1270	4 ₃ 6 ₁	4 ₁ 6 ₁ + 636
1677	6 ₄	6 ₂ + 822	1292	6 ₄	4 ₂ + 644
1791	3 ₂ 4 ₂	3 ₂ + 759	1313	2 ₁ 4 ₁	2 ₁ + 302
1816	3 ₂ 4 ₁ 6 ₁	3 ₂ + 784	1333	2 ₁ 6 ₁	2 ₁ + 322
1864	2 ₁ 3 ₁	2 ₁ + 517	1417	3 ₃	3 ₂ + 466
2048	3 ₄	3 ₃ + 506	1486	2 ₁ 3 ₁	2 ₁ + 475
2105	3 ₁ 4 ₄	4 ₄ + 473	1544	3 ₂ 4 ₂	3 ₁ 4 ₂ + 452
2120	3 ₁ 4 ₃ 6 ₁	4 ₃ 6 ₁ + 473	1577	3 ₂ 4 ₁ 6 ₁	3 ₁ 4 ₁ 6 ₁ +470
2156	3 ₁ 6 ₄	6 ₄ + 479	1583	3 ₂ 6 ₂	3 ₁ 6 ₂ + 465
2171	2 ₁ 4 ₂	2 ₁ + 824	1637	2 ₁ 4 ₂	2 ₁ + 626
2183	2 ₁ 4 ₁ 6 ₁	2 ₁ + 836	1659	2 ₁ 4 ₁ 6 ₁	2 ₁ + 648
2214	2 ₁ 6 ₂	2 ₁ + 867	1667	2 ₁ 6 ₂	2 ₁ + 656
2286?	---	---	1737	3 ₁ 4 ₄	4 ₄ + 482
2376	2 ₁ 3 ₂	3 ₂ + 1344	1745	3 ₁ 4 ₃ 6 ₁	4 ₃ 6 ₁ + 475
2464	4 ₆	4 ₄ + 832	1759	3 ₁ 6 ₄	6 ₄ + 467
2499	6 ₆	6 ₄ + 822	1765?	---	---
2550	3 ₅	3 ₄ + 502	1878	3 ₄	3 ₃ + 461
2581?	---	---	1952	2 ₁ 3 ₂	2 ₁ 3 ₁ + 466
2658	2 ₁ 3 ₁ 4 ₂	2 ₁ 3 ₁ + 794	1997?	---	---
2673	2 ₂	2 ₁ + 1326	2007	2 ₂	2 ₁ + 996
2685?	---	---	2020	3 ₃ 4 ₂	3 ₃ + 602
2708	2 ₁ 3 ₁ 4 ₂	2 ₁ 3 ₁ + 844	2097?	---	---
2885	2 ₁ 3 ₃	2 ₁ 3 ₂ + 509	2108	2 ₁ 3 ₁ 4 ₂	2 ₁ 3 ₁ + 622
2971	2 ₁ 4 ₄	4 ₄ + 1339	2123	2 ₁ 3 ₁ 4 ₁ 6 ₁	2 ₁ 3 ₁ + 637
2994	2 ₁ 4 ₃ 6 ₁	4 ₃ 6 ₁ + 1347	2145	2 ₁ 3 ₁ 6 ₂	2 ₁ 3 ₁ + 659
3008	2 ₁ 6 ₄	6 ₄ + 1331	2258?	---	---
3021?	---	---	2331?	---	---

This is the author's peer reviewed, accepted manuscript. However, the online version of record will be different from this version once it has been copyedited and typeset.
PLEASE CITE THIS ARTICLE AS DOI: 10.1063/5.0182504

3152?	---	---		2351?	---	---
3195	2_23_1	$2_2 + 522$		2409	2_13_3	$2_13_2 + 457$
3393	2_13_4	$3_4 + 1345$		2483	2_23_1	$2_2 + 476$
3484	2_24_2	$2_2 + 811$		2620?	---	---
3516	$2_24_16_1$	$2_2 + 843$		2631	2_24_2	$2_2 + 624$
3538	2_26_2	$2_2 + 865$		2664	2_26_2	$2_2 + 657$
3956?	---	---		2670?	---	---
3973	2_3	$2_2 + 1300$		2697?	---	---
				2723?	---	---
				2763?	---	---
				2947	2_23_2	$2_23_1 + 464$
				2988	2_3	$2_2 + 981$
				3379?	---	---
				3398?	---	---
				3449	2_33_1	$2_3 + 461$
				3470?	---	---
				3612?	---	---
				3662?	---	---
				3962	2_4	$2_3 + 974$
				4430	2_43_1	$2_4 + 468$
				4468?	---	---
				4925	2_5	$2_4 + 963$

This is the author's peer reviewed, accepted manuscript. However, the online version of record will be different from this version once it has been copyedited and typeset.

PLEASE CITE THIS ARTICLE AS DOI: 10.1063/5.0182504

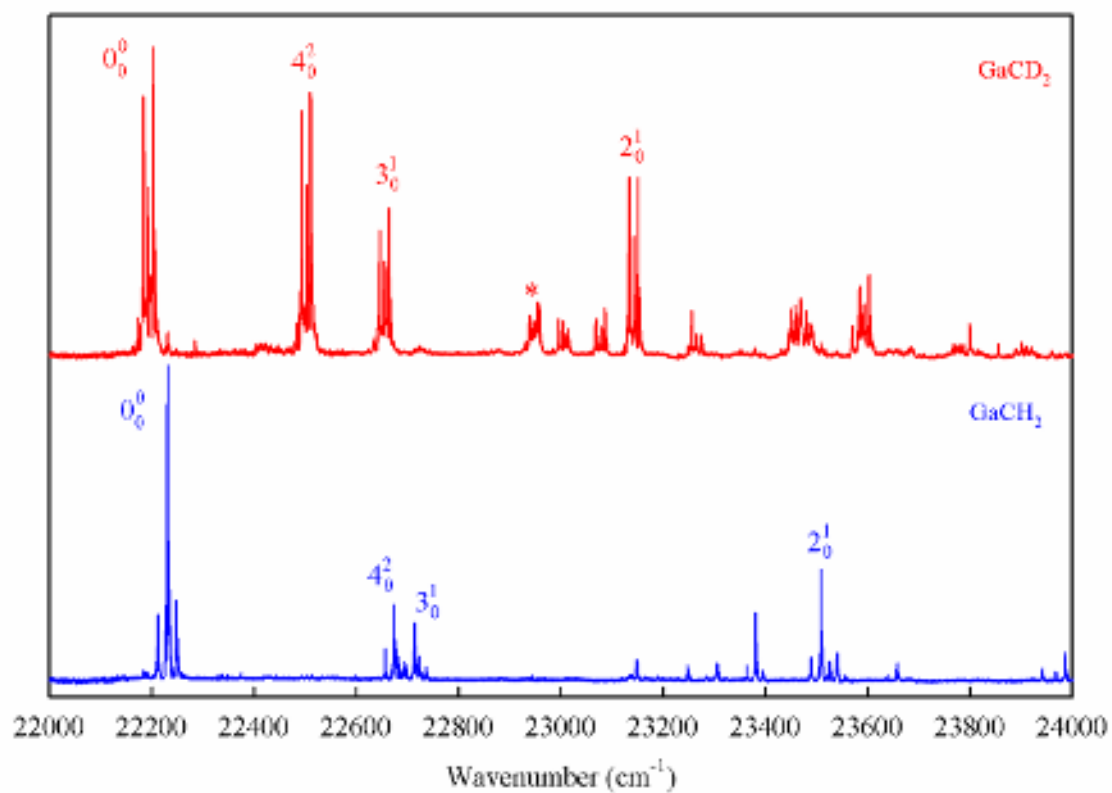


FIG. 7. The medium resolution LIF spectra of GaCD₂ (top) and GaCH₂ (bottom). These spectra were recorded over three laser dyes and are uncorrected for laser power or detector efficiency, so the relative intensities are not very meaningful. An asterisk denotes a LIF feature not attributable to gallium methylene.

and their separation in each emission band were diagnostic of the Q -branch being excited by the laser (${}^pQ_1 = 1$ peak, ${}^rQ_0 = 2$ features split by $4A''$, ${}^rQ_1 = 2$ peaks separated by $8A''$ etc.). Careful study of the LIF rotational contours shows that they are all perpendicular bands, indicative of upper state vibrational levels involving $\nu_1 - \nu_3$ and even quantum number combinations of ν_4 and ν_6 (such as 4_0^2 , 6_0^2 and $4_0^1 6_0^1$) as discussed in section IV.C. Vibronically induced parallel bands, such as 6_0^1 , are not evident in our spectra.

Schooled by our analysis of the emission spectra, we then tackled the LIF spectra which are actually quite complicated. Fig. 7 shows that there is a strong band at $+1278/+949\text{ cm}^{-1}$ ($\text{GaCH}_2/\text{GaCD}_2$ displacement above the 0-0 bands at $22\ 221.5/22\ 189.1\text{ cm}^{-1}$), intervals comparable to those calculated for ν_2' ($1368/1015\text{ cm}^{-1}$). The emission spectra give further credence to this assignment as Franck-Condon considerations suggest that “like should emit to like” and both of these bands show strong emission down to 2_1 and 2_2 . The first two bands in the GaCD_2 LIF spectrum occur at $+309$ and $+462\text{ cm}^{-1}$, whereas in GaCH_2 they appear as a pair of overlapping features at $+445$ and $+484\text{ cm}^{-1}$. The $+484/+462\text{ cm}^{-1}$ bands have very similar excited state energies, with only a small H/D isotope shift (22 cm^{-1}) and both emit weakly to 0_0 and strongly to 3_1 , suggesting an assignment of 3_0^1 . *Ab initio* frequencies of $562/526\text{ cm}^{-1}$ and an isotope shift of 35 cm^{-1} are in general accord with experiment. Using the emission spectra as a guide, we were able to follow the anharmonic ν_3' progression out to three members with 3_0^2 emitting strongly to 3_2 and 3_0^3 emitting primarily to 3_3 .

The first LIF bands at $+445/+309\text{ cm}^{-1}$ must involve ν_4' or ν_6' , although the calculated frequency of the latter ($740/553\text{ cm}^{-1}$) is too high to merit serious consideration. The only possible

assignment on energetic grounds is then 4_0^2 , which owes its intensity to the large change in the ν_4 frequency on electronic excitation (Table II). Unfortunately, the emission spectra of these bands are somewhat contradictory. In GaCD_2 4^2 emits strongly to 0_0 , 2_1 and combinations of ν_2 , ν_4 and ν_6 . In GaCH_2 , strong emission occurs to 0_0 , 3_1 and combinations of ν_4 and ν_6 with little activity in ν_2 . We speculate that in GaCH_2 3^1 and 4^2 (perturbed separation = 38 cm^{-1}) are coupled by Fermi resonance which is why 3_1 shows up prominently in the 4^2 emission. In GaCD_2 , these bands are 143 cm^{-1} apart, so Fermi resonance complications are minimized. In any event, the prominence of ν_4'' and ν_6'' combinations in both emission spectra indicates they have the same upper state assignment and that it must involve a non-totally symmetric mode, viz 4_0^2 . This assignment gives $\nu_4' = 223/155\text{ cm}^{-1}$, rather smaller than the *ab initio* values of $337/265\text{ cm}^{-1}$ although the calculated isotope shift (73 cm^{-1}) is in very good agreement with the experimental value of 68 cm^{-1} . We speculate that the neglect of spin-orbit interactions and the nonplanar \tilde{B} state *ab initio* structure both contribute to the mismatch in the observed and calculated out-of-plane bending frequencies.

In the GaCH_2 LIF spectrum, the pattern of bands with low-frequency intervals is repeated above $23\,700\text{ cm}^{-1}$, with weak bands $+433$ (emitting down to 2_1 and 2_13_1) and $+479$ (emitting down to 0_0 and 2_1) cm^{-1} above 2_0^1 , leading to assignments of $2_0^14_0^2$ and $2_0^13_0^1$, respectively. The analogous LIF bands are found in GaCD_2 at $+318$ (emitting down to 2_1 and 2_13_1) and $+451$ (emitting down to 2_2 and 2_23_1) cm^{-1} above 2_0^1 . A further band at $+1585\text{ cm}^{-1}$ above 0_0^0 has prominent emission down to 3_2 and 3_3 and the correct interval to be assigned as $3_0^34_0^2$ [$1287(3^3) + 299(4^2)$]. Finally, there is a weak GaCH_2 band at $+1075\text{ cm}^{-1}$, which has prominent emission down to 3_1 and 2_13_1 , which we assign as $3_0^14_0^2$, although the interval is rather higher than $443(4^2) + 483(3^1) = 926\text{ cm}^{-1}$.

The only remaining unassigned bands in the LIF spectra ($\text{GaCH}_2 = +1152$ and $+1427 \text{ cm}^{-1}$ and $\text{GaCD}_2 = +812$ and 1072 cm^{-1}) are those that show strong emission down to levels involving ν_4 and ν_6 , signaling that the upper states must also involve these modes. The higher energy bands can be assigned with confidence as 6_0^2 , giving GaCH_2 : $\nu'_6 = 714 \text{ cm}^{-1}$ (*ab initio* = 740 cm^{-1}) and GaCD_2 : $\nu'_6 = 536 \text{ cm}^{-1}$ (*ab initio* = 553 cm^{-1}) and a theoretical H/D isotope shift of 188 cm^{-1} , very close to the experimental value of 178 cm^{-1} . There is a further GaCD_2 band at $+1386 \text{ cm}^{-1}$, with a similar emission spectrum, that can be identified as $4_0^2 6_0^2$ [$1072 (6^2) + 314 (4^2) \text{ cm}^{-1}$].

At this point, the only fly in the ointment is the identity of the medium intensity bands at $+1152$ (GaCH_2) and $+812$ (GaCD_2) cm^{-1} . Both show strong emission down to the 4_2 , $4_1 6_1$ and 6_2 cluster of levels and it is likely that they have the same upper state. The only excited state levels not involving ν'_4 or ν'_6 in this locale, assuming negligible anharmonicity, are 4^4 ($890/618 \text{ cm}^{-1}$), $4^1 6^1$ ($936/690 \text{ cm}^{-1}$) and $4^2 6^1$ ($1158/845 \text{ cm}^{-1}$). Although the latter is energetically realistic, our previous discussion of the emission spectra showed that vibronically induced transitions involving 6^1 should follow *a*-type selection rules whereas both LIF features are unequivocally perpendicular bands. A $4_0^1 6_0^1$ assignment, involving *c*-type bands, would solve the difficulty but the energy mismatch is unreasonably large. Either the energy level structure in the upper state is substantially perturbed in some fashion or $4_0^1 6_0^2$ gains intensity through some more involved mechanism. We were unable to come to a resolution on this point so have simply included both possibilities in our list of assignments. The assignments, band origins, major emission features, separations from the 0-0 band and summary comments on each LIF band are presented in Table IV.

TABLE IV: Assignments and approximate band origins (cm^{-1}) of the LIF bands of GaCH_2 and GaCD_2 .

GaCH_2				GaCD_2		
Assignment	T_0^a	Emits strongly to	Comments	T_0^b	Emits strongly to	Comments
0_0^0	22 221.5	$0_0, 2_1$		22 189.1	$0_0, 2_1$	H/D shift = 32.4
4_0^2	22 666.6	$0_0, 3_1, 4_4$	+445.1 [$\nu'_4 = 222.6$]	22 498.1	$0_0, 2_1, 2_{14_1}$	+309.0 [$\nu'_4 = 154.5$]
3_0^1	22 705.0	$3_1, 2_1, 2_{13_1}$	+483.5 [$\nu'_3 = 483.5$]	22 650.8	$3_1, 2_1, 2_{13_1}$	+461.7 [$\nu'_3 = 461.7$]
3_0^2	23 139.6	3_2	+918.1 [$3_0^1 + 434.6$]	23 074.1	3_2	+885.0 [$3_0^1 + 423.3$]
$3_0^1 4_0^2?$	23 296.6	$3_1, 2_{13_1}$	+1075.1 [$3_0^1 + 591.6$]	--	---	---
$4_0^1 6_0^1 / 4_0^1 6_0^2$	23 373.2	$4_2, 4_6$	+1151.7 [$6^1 + 437$]	23 001.0	$6_2, 4_{16_1}$	+811.9 [$6^1 + 276.1$]
2_0^1	23 499.2	$2_1, 2_2$	+1277.7 [$\nu'_2 = 1277.7$]	23 138.0	$2_1, 2_2$	+948.9 [$\nu'_2 = 948.9$]
3_0^3	23 531.8	3_3	+1310.3 [$3_0^2 + 392.2$]	23 475.9	3_3	+1286.8 [$3_0^2 + 401.8$]
6_0^2	23 648.0	$4_{16_1}, 4_4$	+1426.5 [$\nu'_6 = 713.3$]	23 260.7	$4_2, 4_{16_1}$	+1071.6 [$\nu'_6 = 535.8$]
$4_0^2 6_0^2?$	---	---	---	23 574.9	$4_2, 4_{16_1}, 6_2$	+1385.8 [$6_0^2 + 314.2$]
$2_0^1 4_0^2$	23 932.5	2_{13_1}	+1711 [$2_0^1 + 433.3$]	23 455.5	$2_1, 2_{13_1}, 2_2$	+1266.4 [$2_0^1 + 317.5$]
$2_0^1 3_0^1$	23 978.1	$0_0, 2_1$	+1756.6 [$2_0^1 + 478.9$]	23 589.4	$2_2, 2_{23_1}$	+1400.3 [$2_0^1 + 451.4$]
$3_0^3 4_0^2$	--	--	--	23 774.5	$3_2, 3_3$	+1585.4 [$3_0^3 + 298.6$]

^aFor GaCH_2 , T_0 calculated as pQ_I maximum + $(A - \bar{B})'' = 10.00 \text{ cm}^{-1}$ or rQ_0 maximum - $(A - \bar{B})' = 9.33 \text{ cm}^{-1}$.

^cFor GaCD_2 , T_0 calculated as pQ_I maximum + $(A - \bar{B})'' = 4.87 \text{ cm}^{-1}$.

V. DISCUSSION

A. Ground state molecular structure and vibrational frequencies

We can compare our *ab initio* values of the GaCH₂ ground state structure to similar values from the literature. For trimethylgallium, the experimental bond lengths from a gas-phase electron diffraction study³¹ are Ga-C = 1.967 ± 0.002 Å and C-H = 1.0821 ± 0.003 Å, only slightly shorter than our best IC-MRCI [aug-cc-pwCVTZ, d-electrons correlated] calculated values (2.013 and 1.093 Å). The ground-state bond length of GaC (⁴Σ) is presently unknown but the best calculated³² equilibrium value [CASSCF/MRCI, aug-cc-pV5Z basis set] is 2.025 Å, consistent with our predictions (2.010 - 2.040 Å, Table II) for GaCH₂.

Our experimentally determined ground state Ga-C stretching frequencies (ν_3'') are 517/478 cm⁻¹ (GaCH₂/GaCD₂), in general accord with the Ga-C frequencies of Ga(CH₃)₃/Ga(CD₃)₃ obtained from IR and Raman studies³³ as 527/478 cm⁻¹. For GaC, the calculated ground state vibrational fundamental³¹ is 549 cm⁻¹, only slightly larger than the GaCH₂ value. The experimentally determined CH₂ symmetric bending frequencies of aluminum methylene³ (1353/1016) and gallium methylene (1347/1011) are virtually identical, suggesting that the methylene group is only mildly perturbed by the metal atom.

B. Comparison of the excited state properties of AlCH₂ and GaCH₂

Table V shows a comparison of the changes in geometric structure and vibrational frequencies for the various AlCH₂ and GaCH₂ excited states derived from *ab initio* theory and the available experimental data. The low-lying \tilde{A}^2A_1 states are a result of promoting an electron from the metal-based lone pair *s* orbital to an out-of-plane *2p* orbital on carbon, yielding a •M=CH₂ structure. In both molecules, this results in a substantial decrease in the metal-carbon bond length

and a concomitant increase in the HCH angle. The $\tilde{A} - \tilde{X}$ transitions of both radicals occur in the near infrared in a region which will be difficult to interrogate with conventional LIF or emission techniques. The changes in vibrational frequencies are as expected with a decrease in ν_2 and an increase in ν_3 on electronic excitation.

The \tilde{B} state is formed by promotion of an electron from the lone pair s orbital on the metal to the empty lowest unoccupied molecular orbital, with only minor changes in the molecular structure, including an approximately 5° increase in the HCH angle. The GaCH_2 excited state is almost $3\,000\text{ cm}^{-1}$ higher in energy than AlCH_2 and this may account for the slightly different behavior of the vibrational frequencies on electronic excitation in the two radicals.

An interesting aspect of the present work concerns the *ab initio* finding that the \tilde{B} state has a nonplanar structure. The experimental data suggest that, if there is some nonplanarity, it is slight, as evidenced by the fact that the 4_0^1 bands are so weak in emission. However, a flat or distinctly anharmonic excited state out-of-plane bending potential would probably explain the difficulties we had in assigning the LIF spectrum based on our expectation of only slightly anharmonic progressions. This aspect of the GaCH_2 excited state awaits the day when rotationally resolved spectra can be obtained and the excited state structure can be derived from such data.

VI. CONCLUSIONS

The GaCH_2 and GaCD_2 free radicals have been detected spectroscopically for the first time as products of an electric discharge through trimethylgallium vapor in high pressure argon. The electronic transition at 450 nm detected by LIF spectroscopy has been assigned as $\tilde{B}^2A_2 - \tilde{X}^2B_1$ based on the high-level *ab initio* calculations reported in this work, the observed H/D isotope and nuclear statistical weight effects in the spectra, and the correspondence with the electronic spectra

This is the author's peer reviewed, accepted manuscript. However, the online version of record will be different from this version once it has been copyedited and typeset.

PLEASE CITE THIS ARTICLE AS DOI: 10.1063/5.0182504

of AlCH_2 . Four of the six vibrational frequencies (ν_2 , ν_3 , ν_4 and ν_6) have been established in the \tilde{X} and \tilde{B} electronic states of GaCH_2 and GaCD_2 . The observed LIF and emission spectra provide sensitive methods of detecting and monitoring the gallium methylene free radicals in the gas phase.

TABLE V. Comparison of the ground state molecular structures, band origins and vibrational frequencies and their changes on electronic excitation for MCH_2 ($X = Al, Ga$) molecules.

\tilde{X}^2B_1 Ground State							
	$r(M-C)$ Å	$r(C-H)$ Å	$\theta(HCH)$ °	T_0 (cm^{-1})	ν_2 (cm^{-1}) CH ₂ bend	ν_3 (cm^{-1}) M-C stretch	Source
AlCH₂	1.959	1.106	110.4	0	1353	612	Expt. Ref. 3
GaCH₂	2.013 ^a	1.093 ^a	110.9 ^a	0	1347 ^b	517 ^b	This work
\tilde{A}^2A_1 Excited State							
	$\Delta r(M-C)$ Å	$\Delta r(C-H)$ Å	$\Delta\theta(HCH)$ °	T_0	$\Delta\nu_2$	$\Delta\nu_3$	Source
AlCH₂	-0.128	-0.019	+8.0	6533	-109	+148	Theory. Ref. 2
GaCH₂	-0.177 ^a	-0.010 ^a	+11.5 ^a	6847 ^a	-103	+176	This work.
\tilde{B}^2A_2 Excited State							
	$\Delta r(M-C)$ Å	$\Delta r(C-H)$ Å	$\Delta\theta(HCH)$ °	T_0	$\Delta\nu_2$	$\Delta\nu_3$	Source
AlCH₂	-0.016	-0.015	+5.0	19 572	+24	+51	Expt. Ref. 3
GaCH₂	-0.042 ^a	-0.006 ^a	+4.3 ^a	22222 ^b	-70 ^b	-34 ^b	This work.

^a Theory. Table II, slightly nonplanar geometry in the \tilde{B} state.

^bExperiment.

SUPPLEMENTARY MATERIAL

See the supplementary material for a plot of the GaCH₂ molecular orbitals and pdf copies of the extensive emission spectra recorded during the course of this work.

ACKNOWLEDGEMENTS

The authors thank Crystal Stover for proofreading the manuscript. R.T. acknowledges financial support from the University of Bologna. This research was funded by Ideal Vacuum Products.

AUTHOR DECLARATIONS

Conflict of Interest

The authors have no conflicts to disclose.

Author Contributions

Tony. C. Smith: Conceptualization, data acquisition and analysis, funding acquisition.

Riccardo Tarroni: *Ab initio* calculations, data analysis, manuscript writing and editing. **Dennis**

Clouthier: Conceptualization, data acquisition and analysis, manuscript writing and editing.

DATA AVAILABILITY

The data that support the findings of this study are available within the article and in the supplementary material.

References

1. T. J. Mountziaris and K. F. Jensen, J. Electrochem. Soc. **138**, 2426 (1991).
2. R. Tarroni and D. J. Clouthier, J. Chem. Phys. **153**, 014301 (2020).
3. F. X. Sunahori, T. C. Smith and D. J. Clouthier, J. Chem. Phys. **157**, 044301 (2022)
4. H. Harjanto, W.W. Harper, and D. J. Clouthier, J. Chem. Phys. **105**, 10189 (1996).
5. W. W. Harper and D. J. Clouthier, J. Chem. Phys. **106**, 9461 (1997).
6. D. L. Michalopoulos, M. E. Geusic, P. R. R. Langridge-Smith, and R. E. Smalley, J. Chem. Phys. **80**, 3556 (1984).
7. T. C. Smith, M. Gharaibeh and D. J. Clouthier, J. Chem. Phys. **157**, 204306 (2022).
8. L. I. Zakharkin, V. V. Gavrilenko and N. P. Fatyushina, Russ. Chem. Bull. **46**, 379 (1997).
9. G. A. Atiya, A. S. Grady, D. K. Russell and T. A. Claxton, Spectrochim. Acta., **47A**, 467 (1991).
10. Molpro, version 2010.1, a package of ab initio programs, H. -J. Werner, P. J. Knowles, and others, see <https://www.molpro.net>.
11. CFOUR, version 1.0, a quantum-chemical program package, J. F. Stanton, J. Gauss, L. Cheng, M.E. Harding, D.A. Matthews, P.G. Szalay, and others, See <http://www.cfour.de>.
12. H.-J. Werner and P. J. Knowles, J. Chem. Phys. **82**, 5053 (1985)
13. P. J. Knowles and H.-J. Werner, Chem. Phys. Lett. **115**, 259 (1985).
14. H.-J. Werner and P. J. Knowles, J. Chem. Phys. **89**, 5803 (1988).
15. P. J. Knowles and H.-J. Werner, Chem. Phys. Lett. **145**, 514 (1988).
16. E. R. Davidson and D. W. Silver, Chem. Phys. Lett. **52**, 403 (1977).
17. H.-J. Werner, M. Kállay, and J. Gauss, J. Chem. Phys. **128**, 034305 (2008).
18. J. F. Stanton and J. Gauss, Adv. Chem. Phys. **125**, 101 (2003).

19. K. Raghavachari, G.W. Trucks, J.A. Pople and M. Head-Gordon, Chem. Phys. Lett. **157**, 479 (1989).
20. J. F. Stanton and R.J. Bartlett, J. Chem. Phys. **98**, 7029 (1993).
21. J. F. Stanton and J. Gauss, Theor. Chim. Acta **91**, 267 (1995).
22. A. K. Wilson, D. E. Woon, K. A. Peterson, T. H. Dunning, J. Chem. Phys. **110**, 7667 (1999).
23. T. H. Dunning, J. Chem. Phys. **90**, 1007 (1989).
24. K. A. Peterson and T.H. Dunning, Jr., J. Chem. Phys. **117**, 10548 (2002).
25. N. J. DeYonker, K. A. Peterson and A. K. Wilson, J. Phys. Chem. A **111**, 11383 (2007).
26. F. L. Pilar, *Elementary Quantum Chemistry*, 2nd edition, Dover, 2003.
27. D. G. Fedorov, S. Koseki, M. W. Schmidt and M. S. Gordon, Int. Rev. Phys. Chem. **22**, 551 (2003).
28. PGOPHER, A Program for Simulating Rotational, Vibrational and Electronic Spectra, C. M. Western, *Journal of Quantitative Spectroscopy and Radiative Transfer*, **186** 221-242 (2016).
29. D. J. Clouthier and D. A. Ramsay, Annu. Rev. Phys. Chem. **34**, 31 (1983).
30. J. Coon, R. E. DeWames, and C. M. Lloyd, J. Mol. Spectrosc. **8**, 285 (1962).
31. B. Beagley, D. G. Schmidling and I. A. Steer, J. Mol. Struct. **21**, 437 (1974).
32. G. F. S. Fernandes, M. A.P. Pontes, M. H. de Oliveira, L. F.A. Ferrão and F. B.C. Machado, Chem. Phys. Lett. **687**, 171 (2017).
33. D. C. McKean, G. P. McQuillan, J. L. Duncan, N. Shephard, B. Munro, V. Fawcett and H. G. M. Edwards, Spectrochim. Acta, **43A**, 1405 (1987).